




# Thermal characterization and rheological behavior of some varnishes and paints used for wood protection

A. Mihăilă<sup>1</sup> · M. Danu<sup>1,2</sup> · C. Ibănescu<sup>1</sup> · I. Anghel<sup>3</sup> · I. -E. Șofran<sup>3</sup> · L. V. Balanescu<sup>3</sup> · N. Tudorachi<sup>2</sup> · G. Lisa<sup>1</sup> 

Received: 18 January 2021 / Revised: 26 May 2021 / Accepted: 25 July 2021 / Published online: 5 August 2021  
© Islamic Azad University (IAU) 2021

## Abstract

They were analyzed the thermal and rheological behavior of several varnishes and paints, used for wood protection, available on the market. The thermogravimetric analysis coupled with mass spectrometry and Fourier transform infrared spectrometry technique revealed that the degradation mechanism is complex and includes two to five decomposition stages depending on the composition. The analysis of the gases resulting from the decomposition processes of the water-based samples showed that carbon dioxide was the main potentially harmful product, whereas for those containing solvent these harmful agents were as follows: benzene, xylene and carbon dioxide. The decomposition of the sample containing urea-alkyd resins also results in hydrocyanic acid. The rheological tests showed a viscoelastic solid behavior in the case of water-based film-forming products, and a viscoelastic liquid behavior in the case of solvent-based ones. The microscale combustion calorimetry technique confirmed that this sample has the lowest thermal stability and can contribute the most to the triggering of fires.

---

Editorial Responsibility: S. Mirkia.

---

✉ G. Lisa  
gapreot@yahoo.com; gapreot@ch.tuiasi.ro

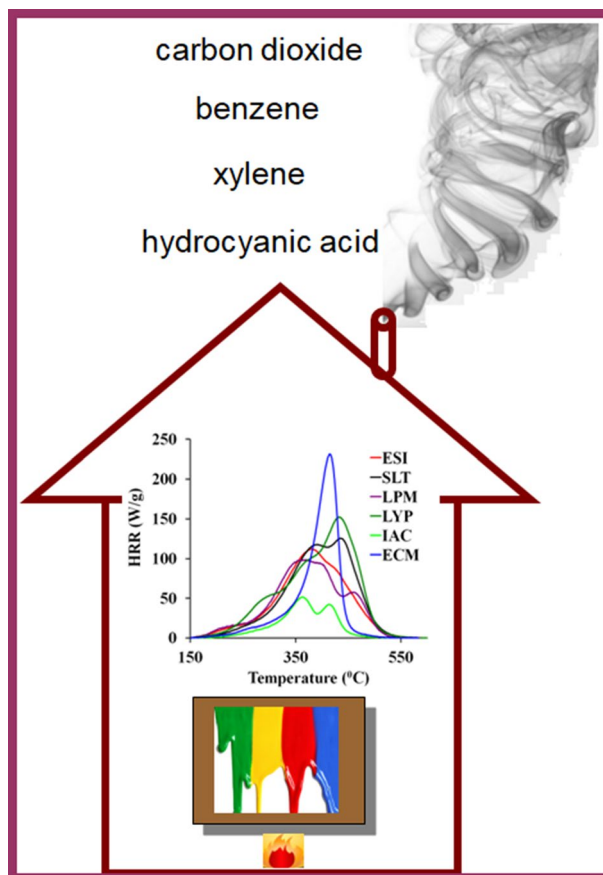
<sup>1</sup> Faculty of Chemical Engineering and Environmental Protection “Cristofor Simionescu”, Gheorghe Asachi Technical University of Iasi, Bd. Mangeron 73, 700050 Iasi, Romania

<sup>2</sup> Petru Poni Institute of Macromolecular Chemistry, 41A Aleea Gr. Ghica Voda, 700487 Iasi, Romania

<sup>3</sup> Fire Officers Faculty, Police Academy “Alexandru Ioan Cuza”, Str. Morarilor 3, Sector 2, 022451 Bucharest, Romania



## Graphic abstract



**Keywords** Varnishes and paints · Thermogravimetric analysis · Mass spectrometry · Fourier transform infrared spectrometry · Rheological behavior · Microscale combustion calorimetry

## Introduction

Wood has been used extensively both in refurbishing existing dwellings and also in the construction of new dwellings. This building material meets current requirements for energy efficiency and optimum indoor air quality. It can also help significantly reduce the noise level for additional comfort.

In order to enjoy these advantages of wooden buildings for as long as possible, they must be properly treated with different types of varnishes and paints. Varnishes and paints are complex systems that consist of three main components, namely a liquid phase (consisting of water or organic solvent), a polymer used to form the film and pigments. Paints also contain additives that contribute to the improvement of their properties. The components of any paint must be in proper quantities so as to obtain finished products with suitable viscosity to allow their storage in containers. They must also be easily transferable from

the container in which they are stored and applied to the surface to be protected, and form a weather-resistant film which enhances shine, color and protection (Hester and Squire 1997). Viscosity is a very important property of coating products. Performing tests on how paints behave during storage and application is closely related to determining the dependence between viscosity and the shear phenomenon and to assessing changes in viscosity and viscoelastic properties during the shear phenomenon, respectively (Deka and Dey 2013). During paint application by brush or roll, a minimum shear effect must be achieved, the paint must be easy to apply without affecting the flow of the paint and the degree of coverage. Paint application must be carried out in such a way as to obtain even coating without runoff due to gravity. In essence, a paint must be a solid that becomes a viscous liquid when applied and which solidifies back at constant rate, which is low enough to allow achieving an even coating. At the same time, the dry rate should be fast enough to prevent paint runoff on



vertical surfaces due to gravity. Special attention must be paid to the rheological characteristics in order to obtain a resistant paint film and appropriate behavior during storage and application. All these requirements that must be met are checked by rheological measurements conducted in varnish and paint factories. These measurements are very important in the process of finding and formulating new coating products (Deka and Dey 2013; Eley 2005). Water-based paints are preferred due to their reduced environmental impact, to the fact that they are odorless and also to their simple application method. However, from a rheological point of view, solvent-based paints are preferred because water-based paints may exhibit lower flow and drying rate than solvent-based paints. In order for water-based paints to act in the same way as solvent-based paints, rheological modifiers need to be added. Thickening agents are used to obtain higher viscosities at high shear rates with good results in obtaining proper paint films. If both viscosity and shear are lower, better flow, faster drying and better shine are achieved. The successful application of the coating product and the formation of the paint film depends on ensuring a high degree of flow control. Understanding and controlling the rheological aspects is very important when analyzing and characterizing some coating products. Studies have concluded that more than half of the costs related to the formulation of a new product recipe is spent on achieving correct rheological characteristics (Eley 2005).

Another important aspect that should be considered when choosing a coating product for wood protection is its thermal behavior. The thermogravimetric analysis, coupled with mass spectrometry and Fourier transform infrared spectrometry (TG/MS/FTIR) technique applied to different types of varnishes and paints provides information on their composition and also on potentially harmful degradation products that may result during the thermal decomposition process in an inert or oxidative atmosphere. Tao L. et al. applied the thermogravimetric analysis (TG) technique coupled with Fourier transform infrared spectrometry (FTIR) to describe the pyrolysis process of some paint and slag waste (Thao et al. 2010). The results that it obtained revealed the existence of three stages in the pyrolysis process. The authors conducted tests at different heating rates, different waste particle sizes and different final temperatures in order to investigate the characteristics of pyrolysis and gas composition. They identified the presence of carbon monoxide, carbon dioxide, ammonia, methane, nitric oxide, hydrocyanic acid and other alkanes with different lengths of the carbon chain. Ploeger R. et al. used pyrolysis–gas chromatography–mass spectrometry (Py-GC–MS) or thermally assisted hydrolysis and methylation (THM)-GC–MS for the analysis of some commercial artists' alkyd paints (Ploeger et al. 2010, 2008). The pyrolysis–gas chromatography–mass spectrometry (Py-GC–MS)

technique was also used by Scalarone D. and Chiantore O. to characterize some acrylic emulsion paints (Scalarone and Chiantore 2008). Please note that we have not found any literature studies that use the TG/MS/FTIR technique to characterize different types of commercial paints in oxidative atmosphere.

Another extremely important aspect for the thermal characterization of some varnishes and paints is the study of their fire behavior, which allows us to determine how they may be used indoors in order to have a minimal negative fire safety impact. Using a cone calorimeter, Staggs et al. analyzed the ignition of construction materials such as plywood and chipboard, on which one or more coats of paint were applied (Staggs et al. 2003). They have shown that if the walls and ceiling are lined with wood-based building materials on which two coats of paint have been applied at the most, the ignition time increase is two-fold. When a large number of paint coats is used, the ignition resistance of the analyzed material is significantly reduced, and this may contribute to the much faster spread of the flame in case of a fire. Microscale combustion calorimetry (MCC), which uses a small calorimeter, may be an alternative to cone calorimeter tests. It was developed to assess the heat release properties of different types of polymeric materials. This piece of equipment has proved its usefulness in the analysis of the fire behavior of different types of materials, because it has the advantage of using small amounts of samples (milligrams) for testing (Wilkie et al. 2006). The method simulates sample flame burning by pyrolysis in an  $N_2$  environment, and the resulting gases are then oxidized in an  $O_2$ -rich environment (Lin et al. 2007). Higher heating rates are used to simulate the fire behavior of a material than in thermal analysis. The reason is the need to quickly obtain decomposing gas streams that are mixed in the combustor at 900 °C with a measured amount of oxygen to achieve the heat release rate of volatile agents.

The TG/MS/FTIR technique was used for the first time in this research, on a series of commercial varnishes and paints used for wood protection, in order to obtain information on their thermal stability, but also to identify the resulting degradation products at different temperatures. The research continues with the carrying out of rheological tests to obtain various correlations between paint flow and some specific features of these coatings, such as runoff, coating capacity and behavior after application. The paint and varnish coats formed on wooden surfaces were detached with a cutter and were analyzed for the first time by the microscale combustion calorimetry (MCC) technique. The aim was to determine some important parameters regarding the fire behavior of the analyzed paint and varnish coats, namely: HRC—Heat release capacity; THR—Total heat released; char Yield—Percentage of



residual mass and decomposition rate. The experimental determinations were performed in the period 2019–2020 in laboratories from Romania, in the “Gheorghe Asachi” Technical University of Iasi, “Petru Poni” Institute of Macromolecular Chemistry and “Alexandru Ioan Cuza” Police Academy in Bucharest.

## Materials and methods

### Materials

A number of commercially available varnishes and paints containing water-based or solvent-based alkyd and/or acrylic resins that are recommended by manufacturers for wood protection have been analyzed.

*Yacht lake* (LYP) is a protective lake with very good properties, of ureo-alkidic type. It is a special type of protective coating which contains special components for ensuring a high degree of wood protection. This product is used for varnishing and protect wood surfaces inside and also outside. Inside is used to protect wood structures like boat suprastructures. Outside is used to protect exterior doors and windows, garden furniture, cottages, railings and fences. It is an resistant product due to the urethanic component which confers a hard and shiny film with a high resistance to the weather conditions and abrasion. Also is a very good and useful product thanks to the next aspects: drying process is fast, adhesion on wood surface is very good. An aspect which can be mentioned is that the product doesn't contain lead and has very good and durable results. The specification sheet and the safety data sheet indicate the presence of medium aliphatic naphtha solvent (petroleum), xylene in a concentration of between 25 and 50%, 2-butanone oxime and cobalt bis (diethylhexanoate) in a concentration of less than 1%. The density of the product is 952 kg/m<sup>3</sup>, and the content of non-volatile substances is 57–59%.

*Acrylic impregnant* (IAC) is an impregnation primer water-based which contains biocides and fungicides substances. This product confers protection for all wood types, for every essence including hardwood and softwood. It can be used to protect wood exploited indoor and also outdoor, this aspect is possible thanks to the product properties to penetrate deep into the wood fiber. The impregnant provides microbiological protection and also protect the wood substrate against fungi, molds, insects and blue stains. Also offers protection against the atmospheric factors and also against to the UV radiations. The producer offers information about application process and about the conditions which need to be respected to obtain the desired protection, like an environment relative

humidity of maxim 70%, temperature between 10 and 30°C. Also is very important to know that the product can be applied only if the wood substrate is dry. The product contributes to reduce the phenomenon of drying and swelling of the wood substrate. Water-repellent wood characteristic is achieved using the impregnant in addition to optimize the adhesion between the substrate and the finish applied later. According to the safety data sheet and specification sheet, IAC contains acrylic dispersion, transparent pigment pastes, water, additives, 2-methoxy-methylethoxy propanol and zirconium 2-ethylhexanoate in percentages between 3 and 5%, while 3-Iodo-2-propynyl Butyl Carbamate is present in percentages less than 1%, and permethrin in less than 0.1%. The density of the product is 1020–1040 kg/m<sup>3</sup>, and the content of non-volatile substances is 27–32%.

*The protective lake with teflon* (SLT) is a type of lake which ensures very good results thanks to the teflon used in his composition. Using of this product ensures the formation of a shiny and resistant film, which confers a long time resistance against UV radiations and weather conditions. It can be succesfully used inside and also outside. Teflon offers very good properties of the product, like a high resistance to stain and dirt, in this way, the surfaces can be cleaned easily. This type of lake it is based on alkydic resins, pigments, organic solvents and additives. The protective lake which contains teflon has high resistance to weathering and against the solar radiation action. Also, it can be observed that the product has a good adhesion to the substrate, a wear resistance and also provides protection against moisture. The density of this lacquer containing Teflon is 900–950 kg/m<sup>3</sup>, and the content of non-volatile substances is 58–62%. The specification sheet and safety data sheet show that SLT contains medium aliphatic naphtha solvent (petroleum), hydro-treated heavy naphtha (petroleum), C9-C11 hydrocarbons, N-alkanes, isoalkanes, xylene, less than 2% cyclic aromatic hydrocarbons.

*Water-based ecolasure* (ECM) is a thick lasure which contains water and also it can be observed an addition of pigments resistant at UV radiations, and also at weathering conditions. This product also can be used inside and outside to protect any type of wood, by providing resistance at the atmospheric and biological factors like fungi, mold, blue stains, insects and also after this product application, the wood substrate doesn't swell or contract. Ecolasure contains an UV filter that protects against solar radiation. The formed film is drying fast and ensures wood ignifugation. The specification sheet and safety data sheet show that water-based ecolasure (ECM) contains 1-methoxy-2-propanol in a concentration of less than 2.5%, 1,3-iodo-2-propynyl butyl-carbamate, permethrin, 1,2-benzisothiazole-3(2H)-one in a



concentration of less than 1%. The density is 950–1050 kg/m<sup>3</sup>, and the content of non-volatile substances is 14%.

*Protective lake (LPM)* is an product assimilated to a azure, it can be used for any type and for any essence of wood. It is destined to protect wood inside and also outside, can be used in conditions of high temperature and humidity, conditions that intensifies the microbial attack against the wood substrate. The product penetrate deep into the wood fiber providing a very good and long-term resistance, ensures a high protection of wood against weathering and UV radiations. According to the specification sheet and safety data sheet, the protective lacquer (LPM) contains medium aliphatic naphtha solvent (petroleum), and xylene in a proportion of 10–25%, aromatic hydrocarbons and naphthenes, butan-1-ol in concentrations of 2.5–10%, and in concentrations less than 1%: 3-iodo-2-propynyl butylcarbamate, 2-ethylhexanoic acid, zirconium salt, 2-butanone oxime, cobalt bis (diethylhexanoate) and permethrin. The density of the product is 920–960 kg/m<sup>3</sup>, and the content of non-volatile substances is 57%.

*Super-glossy enamel (ESI)* is an alkydic product based on fatty alkyd resins with multiple application possibilities, like applications on multiple types of surfaces. It can be used to protect and decorate wood surfaces, to protect metal surfaces but also to protect the masonry inside and also outside. The film formed is characterized by a high gloss, a fast dry and also a very good resistance against the weathering, temperature variations and humidity. The product is used in the case of new surfaces and also it can be used successfully in the case of the surfaces that have been painted before. Super-glossy enamel (ESI) has a non-volatile substance content of 52% and a density of 980–1080 kg/m<sup>3</sup>. From the specification sheet and safety data sheet it appears that this product also contains medium aliphatic naphtha solvent (petroleum) in a concentration of 10–25%, xylene in a proportion of 2.5–10%, and cobalt bis (diethylhexanoate), 2-ethylhexanoic acid, zirconium salt, 2-butanone oxime in concentrations less than 1%.

TG/MS/FTIR tests and rheological behavior were used for fresh paints characterization. Microscale combustion calorimetry (MCC) tests were applied to paint films dried under laboratory conditions for 8 weeks and removed from the wood disks using a cutter.

## Equipment and measurements

### TG/MS/FTIR technique

Thermal degradation and evolved gas analyses of the samples were performed using a TG/FTIR/MS system equipped with a thermogravimetric balance model STA 449F1 Jupiter (Netzsch–Germany) coupled online with

spectrophotometer FTIR model Vertex-70 (Bruker) and mass spectrometer model QMS 403C Aëolos (Netzsch). The thermogravimetric analyzer was calibrated on temperature and sensitivity using the melting-point of the standard metals (Hg, In, Sn, Bi, Zn, Al) from –38.5 to 700 °C temperature. Samples mass ranging from 9.2 to 18.5 mg were heated from 25 to 670 °C, with a heating rate of 10 °C/min in air atmosphere of 40 ml/min flow rate. Data collection was carried out with Proteus® software (Netzsch). The gases released during thermal decomposition processes are transferred by two isothermal transfer lines to FTIR and mass spectrometer. The transfer lines are heated to constant temperatures of 190 and 240 °C, respectively. The gases are introduced in TGA-IR external modulus of the FTIR spectrophotometer, and the spectra are recorded on 600–4000 cm<sup>-1</sup> range with a resolution of 4 cm<sup>-1</sup>. The acquisition of FT-IR spectra in 3D size was done with Opus 6.5 software that performs the starting and synchronization of the three apparatus. The mass spectra were recorded under 10<sup>-5</sup> mbar vacuum and electron impact ionization energy of the 70 eV. The acquisition of data was achieved with Aeolos® 3.2 software in the range of m/z = 1–200, measuring time of 0.5 s for one channel.

### Rheological measurements

The rheological tests were performed using a Physica MCR 501 modular rheometer (Anton Paar, Austria) equipped with a Peltier temperature control system. The parallel plate with 50 mm diameter was used for all measurements. All experiments were carried out at 25 °C, and each sample was left to rest on the device for 5 min before starting the rheological test. Three types of oscillatory tests (amplitude sweep, frequency sweep and time test) and two rotational tests (flow curve and time test) were performed for the rheological characterization of the paint samples. The amplitude sweep was performed at constant frequency (10 rad/s) with an amplitude variation within the 0.01–100% range. This test allows the determination of the linear viscoelastic range of the analyzed samples. Frequency sweep was performed at constant amplitude in the linear viscoelastic range with a frequency variation between 0.1 and 100 rad/s. Both oscillatory tests were performed at constant temperature (25 °C). The time oscillation test was performed at constant amplitude (within the linear viscoelastic range) and constant frequency (10 rad/s). Rotational tests (flow tests) were recorded at 25 °C with a shear rate variation within the 0.01–5000 s<sup>-1</sup> range.



## Microscale combustion calorimetry (MCC) technique

The six types of paint and varnish were applied on fir wood boards. After 8 weeks of drying in laboratory conditions (temperature of  $23 \pm 2$  °C and humidity of  $40 \pm 5\%$ ), the paint was removed with a cutter and analyzed by MCC. This technique was developed by researchers to assess the flammability of different types of materials. The tests were performed according to ASTM D7309-2007 (method A), i.e., the degradation of the samples weighing 3.2–4.7 mg in nitrogen atmosphere at a 1 °C/s rate, within the 25–900 °C temperature range. The gases resulting from the combustion were placed in a high temperature combustion furnace (900 °C). The volumetric flow rate and volumetric oxygen concentration of the gas flow leaving the combustion furnace are measured continuously during the test to calculate the heat release rate using oxygen consumption. It should be noted that this standardized method measures the combustion heat of the volatile components in the sample under analysis, but not the solid residue combustion heat. Combustion heat is considered a fire hazard indicator (Method and for Determining Flammability Characteristics of Plastics and Other Solid Materials Using Microscale Combustion Calorimetry, ASTM D, xxxx).

## Results and discussion

### Fresh paints characterization

#### TG/MS/FTIR studies

The TG/MS/FTIR technique in air atmosphere was applied to analyze the thermal stability and to identify the main potentially harmful degradation products resulting from the thermal decomposition of six types of commercial varnishes and paints.

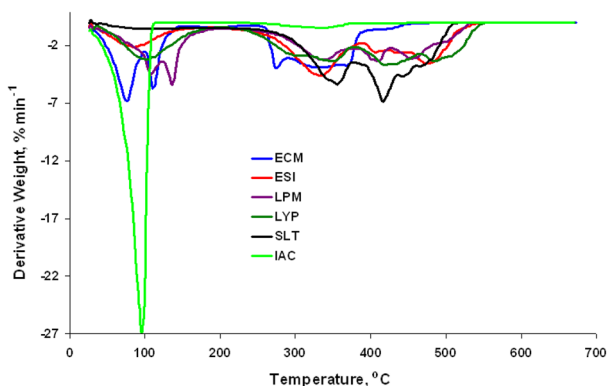


Fig. 1 DTG comparative curves

The DTG (Fig. 1) curves obtained in air reveal that the degradation mechanism is complex and consists of two to five decomposition stages depending on the composition. According to literature (Ploeger et al. 2009; Duce et al. 2014), oxidative decomposition of alkyd resin occurs within the 250–380 °C temperature range, and the degradation rate reaches its peak at about 330 °C ( $T_{\text{peak}}$ ). A peak temperature value ( $T_{\text{peak}} = 331$  °C, 337 °C, 333 °C and 337 °C, respectively) very close to the temperature reported by other researchers was determined for the ECM, LPM, ESI and LYP, which contain alkyd resins. This value is higher by about 20 degrees ( $T_{\text{peak}} = 353$  °C) for commercial paint containing alkyd resins and Teflon (SLT). ECM water-based ecolasure containing both alkyd and acrylic resins underwent a stage corresponding to the oxidative degradation of acrylic components within the 268–300 °C range, with a peak at 275 °C (Crespi et al. 2007; Guo et al. 2018). The volatilization of the organic fraction in paints takes place during the thermal oxidation stages within the 380–560 °C temperature range (Ploeger et al. 2009). According to the DTG curves in Fig. 1, if we disregard the sample water or solvent evaporation stage, we find that the LYP sample containing urea-alkyd resins and the ECM and IAC samples, which also contain acrylic resins, have the lowest thermal stability. The best thermal stability was detected in the SLT sample containing alkyd resins and Teflon. This sample also has the smallest amount of solvent. Water and solvent evaporation takes place up to about 200 °C.

The TG/MS/FTIR technique applied to varnish and paint samples used for wood protection allows the identification of degradation products that result at different temperatures and that can provide information on their components, and also on the risks they put to the environment.

**Water-based alkyd/acryl products (ECM)** The MS spectra obtained at different temperatures for the ECM sample are shown in Figure S1 Supporting Information. The ionic current variation with temperature chart for the  $m/z = 18$  ( $\text{H}_2\text{O}^+$ ) fragment in Fig. 2 proves that water is the predominant solvent in ECM. At temperatures lower than 200 °C within the MS spectrum (figures S1 a and b) of the resulting gases, the  $m/z = 28$  ( $\text{N}_2^+$ ) and  $m/z = 32$  ( $\text{CH}_3\text{OH}^+$ ) fragments were found, which may result from the decomposition of 3-iodo-2-propynyl butylcarbamate and 1-methoxy-2-propanol, which the manufacturer claims are components of this coating product. The presence of the  $m/z = 100$  ( $\text{C}_5\text{H}_8\text{O}_2^+$ ) ionic fragment in the MS spectra at temperatures higher than 200 °C may confirm the existence of the acrylic component in the ECM paint, in other words, it may indicate the presence of the methyl



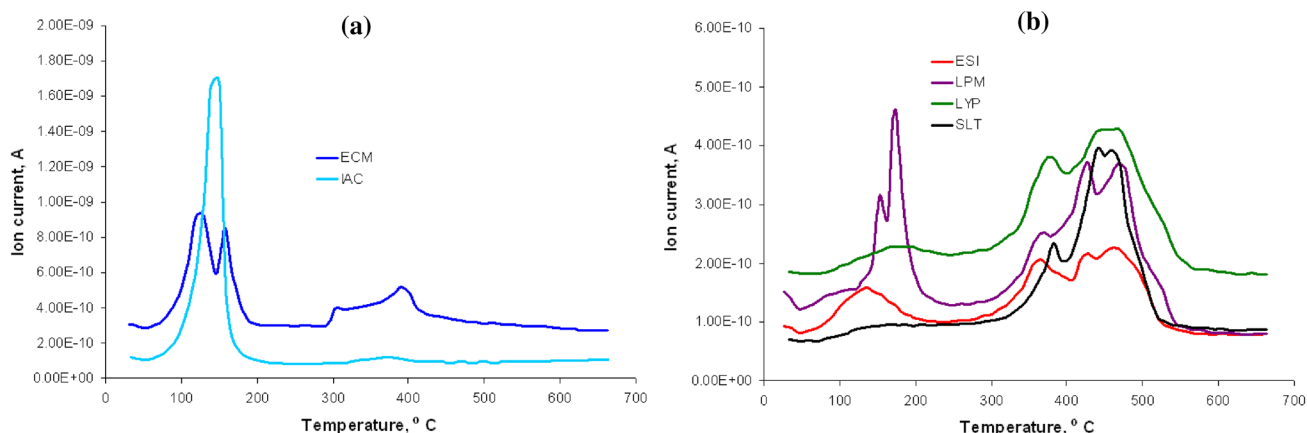


**Fig. 2** Ionic current variation with temperature for the fragments  $m/z = 18$  in air for ECM, IAC (a) and ESI, LPM, LYP, SLT (b)

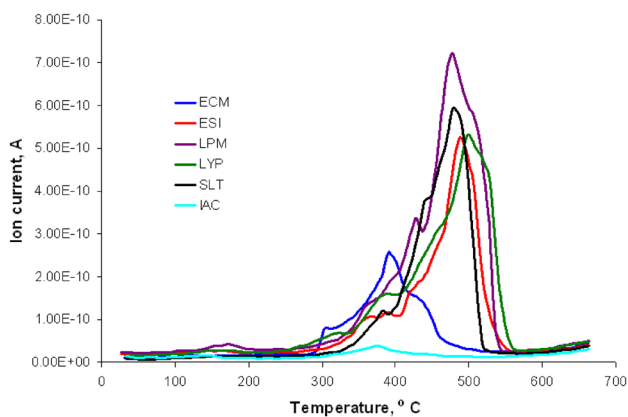


**Fig. 3** Ionic current variation with temperature for the fragments  $m/z = 44$  in air for ECM, ESI, LPM, LYP, SLT and IAC

methacrylate component (Tsuge et al. 1000; Germinario et al. 2016). The intensity of the ionic current was found to be higher in the  $m/z = 91$  ( $C_7H_7^+$ ) fragment at  $364.2^\circ C$ , which indicates the presence of substituted benzene rings in the decomposition gases. The  $m/z = 127$  ionic fragment is also present, which may be associated with the presence of certain naphthalene derivatives ( $C_{10}H_7^+$ ) or iodides ( $I^+$ ). The thermal oxidation process of the organic components present in the ECM paint occurs within the  $268\text{--}500^\circ C$  range, and  $H_2O$  and  $CO_2$  are released (Fig. 2 and Fig. 3).

Additional information about the thermal decomposition of the ECM sample was collected after the analysis of the FTIR spectra for the gaseous phase at different temperatures, shown in Figure S2 Supporting Information. The results obtained are consistent with those established from the analysis of MS spectra. Water-specific bands range

between  $4000\text{--}3500\text{ cm}^{-1}$ , aliphatic structure bands between  $3095\text{--}2886\text{ cm}^{-1}$  (attributed to the C–H stretching vibrations of methylene and methyl groups) and carbonyl compound bands between  $1780$  and  $1660\text{ cm}^{-1}$  (Gawdzik et al. 2019; Worzakowska 2017). Please also note the stretching vibrations of C–O for the  $1170\text{--}1072\text{ cm}^{-1}$  range (Worzakowska 2017) and aromatic compound-specific bands within the  $1590\text{--}1280\text{ cm}^{-1}$  range. The  $931\text{ cm}^{-1}$  peak corresponds to the –N–H bond vibration, which confirms the presence of nitrogen, and the  $2352$  and  $667\text{ cm}^{-1}$  peak correspond to  $CO_2$  (Lisa et al. 2019).

The MS and FTIR spectra obtained from the analysis of gas decomposition in air of water-based alkyd/acrylic resin (ECM) paints indicate carbon dioxide as the major potentially harmful product.

**Water-based acrylic products (IAC)** Water predominates in IAC paints (Fig. 2a). The thermal oxidation of organic components of IAC paints occurs within the  $320\text{--}420^\circ C$  temperature range, and  $H_2O$  and  $CO_2$  are released (Fig. 2a and Fig. 3). Other ionic fragments are not detected. The FTIR spectra obtained at different temperatures for decomposition gases (Fig. 4) reveal water-specific bands between  $4000\text{--}3050\text{ cm}^{-1}$ , aliphatic structure bands between  $3050$  and  $2886\text{ cm}^{-1}$  (attributed to the C–H stretching vibrations of methylene and methyl groups) and  $2352$  and  $667\text{ cm}^{-1}$  peaks corresponding to  $CO_2$  (Lisa et al. 2019). The  $1605$ ,  $1510$  and  $829\text{ cm}^{-1}$  peaks are specific for the aromatic derivatives (Tudorachi and Mustata 2020).

Carbon dioxide was found to be the main potentially harmful product of the decomposition in air of the coating product marked IAC.



**Fig. 4** FTIR spectra of the volatile products evolved during thermal decomposition of IAC

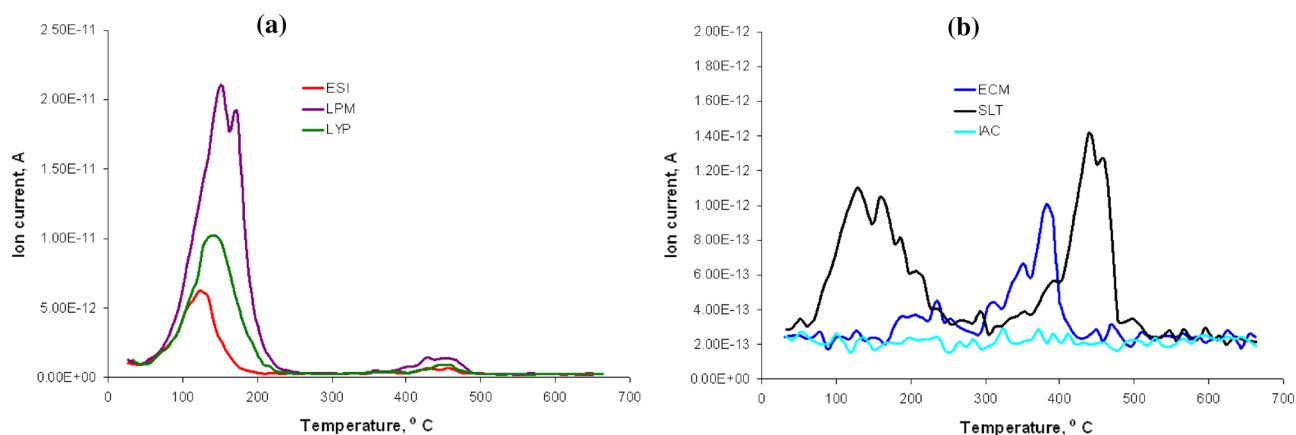
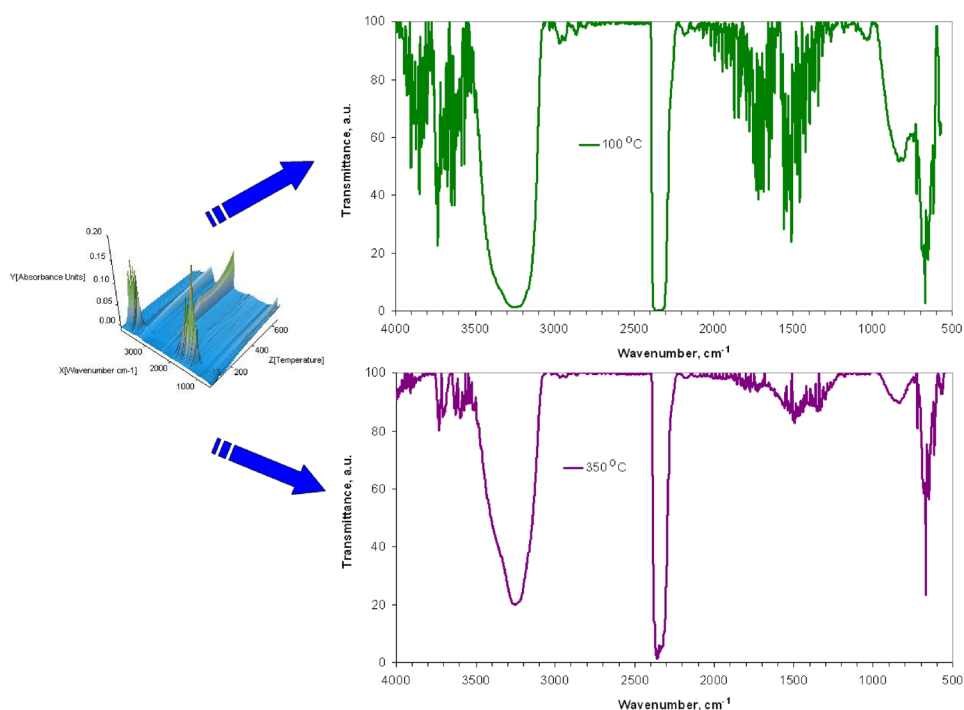


**Fig. 5** Ionic current variation with temperature for the fragments  $m/z=91$  in air for ESI, LPM, LYP (a) and ECM, SLT, IAC (b)

**Solvent-based alkyd products (LPM)** The MS spectra recorded for the LPM sample decomposition gases at different temperatures are shown in Figure S3 Supporting Information. Those corresponding to the first two temperatures confirm the presence of solvent naphtha (petroleum), medium aliphatic declared by the manufacturers, which consists mainly of saturated hydrocarbons with a predominant carbon number ranging between C9 and C12. It also contains aromatic hydrocarbons and naphthenes. According to literature, ionic fragments are obtained from the C–C

splitting of aliphatic chains, grouped in triplets with the general formula  $C_nH_{2n-1}$ ,  $C_nH_{2n}$  and  $C_nH_{2n+1}$  (Lisa et al. 2016). Peaks were detected in  $m/z = 41, 42, 43$  ( $C_3H_5^+$ ,  $C_3H_6^+$ ,  $C_3H_7^+$ ),  $m/z = 55, 56, 57$  ( $C_4H_7^+$ ,  $C_4H_8^+$ ,  $C_4H_9^+$ ),  $m/z = 69, 70, 71$  ( $C_5H_9^+$ ,  $C_5H_{10}^+$ ,  $C_5H_{11}^+$ ),  $m/z = 83, 84, 85$  ( $C_6H_{11}^+$ ,  $C_6H_{12}^+$ ,  $C_6H_{13}^+$ ),  $m/z = 97, 98, 99$  ( $C_7H_{13}^+$ ,  $C_7H_{14}^+$ ,  $C_7H_{15}^+$ ),  $m/z = 111, 112, 113$  ( $C_8H_{15}^+$ ,  $C_8H_{16}^+$ ,  $C_8H_{17}^+$ ),  $m/z = 125, 126, 127$  ( $C_9H_{17}^+$ ,  $C_9H_{18}^+$ ,  $C_9H_{19}^+$ ),  $m/z = 139, 140, 141$  ( $C_{10}H_{19}^+$ ,  $C_{10}H_{20}^+$ ,  $C_{10}H_{21}^+$ ) and  $m/z = 153, 154, 155$  ( $C_{11}H_{21}^+$ ,  $C_{11}H_{22}^+$ ,  $C_{11}H_{23}^+$ ). Please note that the frag-





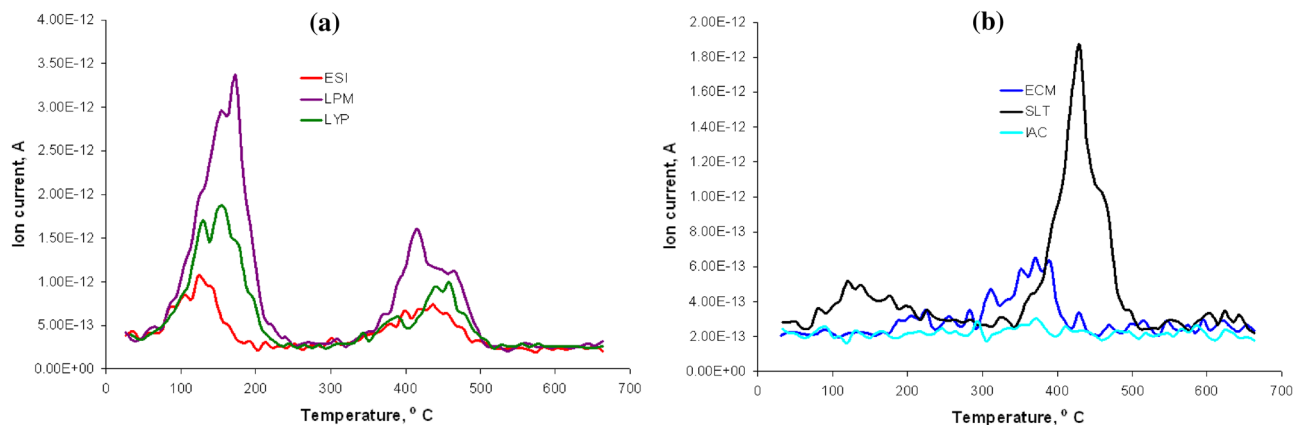


**Fig. 6** Ionic current variation with temperature for the fragments  $m/z=78$  in air for ESI, LPM, LYP (a) and ECM, SLT, IAC (b)

mentation of linear chains caused 14 u.a.m. spaced peaks. The most intense are the  $m/z = 43$  ( $C_3H_7^+$ ) and  $m/z = 57$  ( $C_4H_9^+$ ) peaks, for the other fragments the intensity of the peaks decreases with the increase of the number of carbon atoms from  $n = 5$  to  $n = 11$ .

Figure S3 a and b, Supporting Information, also reveals the presence of  $m/z = 91$  ( $C_6H_5CH_2^+$ ) (Fig. 5),  $m/z = 105$  ( $C_6H_5CH_2CH_2^+$ ) and  $m/z = 119$  ( $C_6H_5CH_2CH_2CH_2^+$ ) fragments, which clearly indicates the presence of a substituted benzene ring. As one may note, their mass increases progressively by 14 u.a.m. According to literature (Hof et al. 2014), the  $m/z = 77, 91, 119$  and  $134$  fragments may be attributed to the presence of *t*-butylphenyl fragments.

According to the derivative thermogravimetric (DTG) curves shown in Figs. 1, the thermal oxidation process starts at temperatures higher than  $300^\circ C$ , and  $H_2O$  and  $CO_2$  are released (Fig. 2 and Fig. 3). As shown in Figure S3c, Supporting Information, the  $m/z = 26$  ( $C_2H_2^+$ ),  $30$  ( $CH_2O^+$ ),  $42$  ( $C_3H_6^+$ ),  $56$  ( $C_4H_8^+$ ) and  $72$  ( $C_4H_8O^+$ ) fragments are also present, and they may result from the decomposition of the alkyd resin in the LPM paint. The  $m/z = 78$  ( $C_6H_6^+$ ) ionic fragment is also added at  $405.9^\circ C$  and  $457.5^\circ C$  (figure S3 d and e Supporting Information), which confirms the presence of benzene in the decomposition gases (Fig. 6).

The FTIR spectra shown in figure S4, Supporting Information, were also recorded for the decomposition gases of the LPM coating product. The first two temperatures, namely  $110$  and  $140^\circ C$ , also showed strong bands that are specific of aliphatic structures between  $3050$  and  $2886\text{ cm}^{-1}$  and of carbonyl compounds between  $1780$  and  $1660\text{ cm}^{-1}$  (Gawdzik et al. 2019; Worzakowska 2017). The aromatic compound-specific bands were also revealed within the  $1590\text{--}1280\text{ cm}^{-1}$  range. The results obtained are consistent with the findings of the MS spectra analysis,

confirming that this type of paint contains mainly solvent naphtha (petroleum), medium aliphatic. The  $2352$  and  $667\text{ cm}^{-1}$  peaks that correspond to  $CO_2$  were also revealed in the FTIR spectra (Lisa et al. 2019), and their intensity increases at temperatures higher than  $300^\circ C$ , when the thermal oxidation process begins. The  $CO$ -specific bands are also present within the  $2200\text{--}2040\text{ cm}^{-1}$  range, while water-specific ones occur between  $4000$  and  $3500\text{ cm}^{-1}$  (Tudorachi and Mustata 2020).

The MS and FTIR spectra of the LPM sample show benzene and xylene as the main potentially harmful products at temperatures below  $300^\circ C$ , and carbon dioxide at higher temperatures.

**Fatty alkyd products (ESI)** At  $100.2^\circ C$ , the MS spectra in Figure S5, Supporting Information, show solvent naphtha (petroleum), medium aliphatic declared by the manufacturers. Ionic fragments were detected resulting from the C–C splitting of aliphatic chains, grouped in triplets with the general formula  $C_nH_{2n-1}$ ,  $C_nH_{2n}$  and  $C_nH_{2n+1}$ , with  $n$  ranging between 3 and 8. The presence of the  $m/z=91$  (Fig. 5),  $m/z=105$  and  $m/z=119$  fragments indicate the presence of a substituted benzene ring, while the  $m/z=77, 91, 119$  and  $134$  fragments may be attributed to the existing *t*-butylphenyl fragments (Hof et al. 2014). At  $343.5^\circ C$  (figure S5b Supporting Information), the  $m/z=26$  ( $C_2H_2^+$ ),  $30$  ( $CH_2O^+$ ),  $39$  ( $C_3H_3^+$ ),  $41$  ( $C_3H_5^+$ ),  $55$  ( $C_4H_7^+$ ),  $67$  ( $C_5H_7^+$ ),  $70$  ( $C_5H_{10}^+$ ) and  $82$  ( $C_6H_{11}^+$ ) also occur, and they may result from the decomposition of the alkyd resin in the ESI varnish. The  $m/z=18$  ( $H_2O^+$ ) and  $m/z=44$  ( $CO_2^+$ ) (Fig. 2 and Fig. 3) fragments are obviously also present, and their intensity increases at  $467.5^\circ C$  (figure S5c Supporting Information).



These findings are also supported by the FTIR spectra obtained from the ESI sample decomposition gases at various temperatures (figure S6 Supporting Information). At 100 °C, we noted strong water-specific bands ranging between 4000 and 3500  $\text{cm}^{-1}$ , aliphatic structure-specific bands between 3050 and 2886  $\text{cm}^{-1}$ , carbonyl compound-specific bands between 1900 and 1650  $\text{cm}^{-1}$ , aromatic compound-specific bands between 1590 and 1280  $\text{cm}^{-1}$ , or alcohol-specific bands between 1000 and 1200  $\text{cm}^{-1}$  (Ma et al. 2018). There are also strong peaks at 2352 and 667  $\text{cm}^{-1}$  corresponding to  $\text{CO}_2$  (Lisa et al. 2019), the intensity of which increases at temperatures higher than 300 °C, when the thermal oxidation process occurs.

The MS and FTIR spectra findings in the ESI sample show benzene and xylene as the main potentially harmful products at temperatures below 300 °C, and carbon dioxide at higher temperatures.

**Urea-alkyd resin varnish (LYP)** The MS spectra obtained for the LYP varnish at different temperatures are shown in Figure S7, Supporting Information. This sample also contains the solvent naphtha (petroleum), medium aliphatic declared by the manufacturers. Thus, as one may note, at the first temperature value, there are ionic fragments resulting from the C–C splitting of aliphatic chains, grouped in triplets with the general formula  $\text{C}_n\text{H}_{2n-1}$ ,  $\text{C}_n\text{H}_{2n}$  and  $\text{C}_n\text{H}_{2n+1}$ , with  $n$  ranging between 3 and 11. At 110.4 °C, the MS spectrum also exhibits the  $m/z = 91$  (Fig. 5),  $m/z = 105$  and  $m/z = 119$  fragments, which indicates the presence of a substituted benzene ring, and also the  $m/z = 77$ , 91, 119 and 134 fragments, which may be attributed to the existence of *t*-butylphenyl fragments (Hof et al. 2014). The  $m/z = 28$  ( $\text{N}_2^+$ ) ionic fragment is also found at this temperature, and it confirms the presence of nitrogen, which may originate in the 2-butanon-oxima declared by the manufacturer. The  $m/z = 26$  ( $\text{C}_2\text{H}_2^+$ ), 30 ( $\text{CH}_2\text{O}^+$ ), 42 ( $\text{C}_3\text{H}_6^+$ ), 56 ( $\text{C}_4\text{H}_8^+$ ) and 72 ( $\text{C}_4\text{H}_8\text{O}^+$ ) fragments occur at 354.2 °C, and they result from the decomposition of the alkyd resin in the LYP paint. From this temperature upward, the ionic current of the  $m/z = 27$  ( $\text{HCN}^+$ ) fragment intensifies, which may be the result, according to literature (Liu et al. 2016; Jiao et al. 2013), of the thermal decomposition of the polyurethane component existing in this type of paint. The  $m/z = 18$  ( $\text{H}_2\text{O}^+$ ) and  $m/z = 44$  ( $\text{CO}_2^+$ ) (Fig. 2 and Fig. 3) also occur at temperatures above 300 °C, which are specific to the thermal oxidation process, but their intensity increase with temperature increase (figure S7b, c and d, Supporting Information). The presence of benzene in decomposition gases is confirmed by ionic current intensification in  $m/z = 78$  ( $\text{C}_6\text{H}_6^+$ ) (see Fig. 6 and figure S7c Supporting Information).

The FTIR spectra of the gaseous phase resulting from LYP sample decomposition are shown at different temperatures in Figure S8, Supporting Information. They are consistent with the observations made based on the analysis of MS spectra. Thus, the FTIR spectrum reveals the following specific bands at 110 °C: for aliphatic structures between 3050 and 2886  $\text{cm}^{-1}$  and for aromatic compounds between 1590 and 1280  $\text{cm}^{-1}$ , which confirms the presence of solvent naphtha (petroleum), medium aliphatic and xylene, declared by the manufacturer. At temperatures higher than 300 °C, the 2352 and 667  $\text{cm}^{-1}$  peaks that correspond to  $\text{CO}_2$  (Lisa et al. 2019) and the water-specific bands between 4000 and 3500  $\text{cm}^{-1}$  are enhanced due to the thermal oxidation process. The 1374  $\text{cm}^{-1}$  peak is specific to the vibration of the (–CN) bond (Spranceana et al. 2017), which may be associated with the presence of HCN, the  $m/z = 27$  ( $\text{HCN}^+$ ) ionic fragment.

According to the MS and FTIR spectra, benzene and xylene are the main potentially harmful products at temperatures below 300 °C, and carbon dioxide and hydrocyanic acid at higher temperatures.

**Products containing alkyds and Teflon (SLT)** Figure S9, Supporting Information, shows the MS spectra obtained for the paint sample marked SLT, at different temperatures. The  $m/z = 14$  ( $\text{N}_2^{++}$ ) and  $m/z = 28$  ( $\text{N}_2^+$ ) fragments clearly prove the presence of nitrogen, and the  $m/z = 16$  ( $\text{O}_2^{++}$ ) and  $m/z = 32$  ( $\text{O}_2^+$ ) fragments the presence of oxygen. At 99.9 °C, the  $m/z = 77$  ( $\text{C}_6\text{H}_5^+$ ),  $m/z = 91$  ( $\text{C}_6\text{H}_5\text{CH}_2^+$ ) (Fig. 5),  $m/z = 105$  ( $\text{C}_6\text{H}_5\text{CH}_2\text{CH}_2^+$ ) and  $m/z = 119$  ( $\text{C}_6\text{H}_5\text{CH}_2\text{CH}_2\text{CH}_2^+$ ) fragments occur, and their mass increases progressively by 14 u.a.m. and clearly indicates the presence of certain aromatic hydrocarbons. The fragments with the general formula  $\text{C}_n\text{H}_{2n-1}$ ,  $\text{C}_n\text{H}_{2n}$  and  $\text{C}_n\text{H}_{2n+1}$ , with  $n$  ranging between 3 and 6, and the  $m/z = 41$ , 42, 43 ( $\text{C}_3\text{H}_5^+$ ,  $\text{C}_3\text{H}_6^+$ ,  $\text{C}_3\text{H}_7^+$ ),  $m/z = 55$ , 56, 57 ( $\text{C}_4\text{H}_7^+$ ,  $\text{C}_4\text{H}_8^+$ ,  $\text{C}_4\text{H}_9^+$ ),  $m/z = 69$ , 70, 71 ( $\text{C}_5\text{H}_9^+$ ,  $\text{C}_5\text{H}_{10}^+$ ,  $\text{C}_5\text{H}_{11}^+$ ),  $m/z = 83$ , 84, 85 ( $\text{C}_6\text{H}_{11}^+$ ,  $\text{C}_6\text{H}_{12}^+$ ,  $\text{C}_6\text{H}_{13}^+$ ) fragments are also present. These fragments confirm the presence of solvent naphtha medium aliphatic. Temperatures higher than 320 °C also see the intensification of the ionic current in the  $m/z = 18$  ( $\text{H}_2\text{O}^+$ ) and  $m/z = 44$  ( $\text{CO}_2^+$ ) (Fig. 2 and Fig. 3) fragments, which are specific to the thermal oxidation processes. Ionic current intensification was also noted in the  $m/z = 50$  ( $\text{CF}_2^+$ ) fragment at temperatures higher than 400 °C, which confirms the presence of Teflon in this coating product.

Figure S10, Supporting Information, shows the FTIR spectra of the SLT sample decomposition gases at various temperatures. Our findings are consistent with the previous ones resulting from MS curve interpretation. Please note the presence of solvent naphtha medium aliphatic

supported by the presence of the aliphatic structure-specific bands between 3050 and 2886  $\text{cm}^{-1}$  and of the aromatic compound-specific bands within the 1590–1280  $\text{cm}^{-1}$  range. Beyond 420  $^{\circ}\text{C}$ , they disappear or diminish significantly. However, we found the 2352 and 667  $\text{cm}^{-1}$  peaks, which correspond to  $\text{CO}_2$ , to intensify (Lisa et al. 2019). The FTIR spectra also show water-specific bands between 4000 and 3500  $\text{cm}^{-1}$ , CO-specific bands within the 2200–2040  $\text{cm}^{-1}$  range and carbonyl compound-specific bands between 1780 and 1660  $\text{cm}^{-1}$  (Gawdzik et al. 2019; Worzakowska 2017). According to literature (Odochian et al. 2014), the presence of the bands ranging from 1305 to 1368  $\text{cm}^{-1}$  may be associated with the C-F bond vibration, which confirms the presence of Teflon in this type of coating product.

MS and FTIR spectra analysis reveals that benzene, xylene and carbon dioxide are the main potentially harmful products in the SLT coating product.

### Rheological behavior

**Amplitude sweep** The viscoelastic behavior of paints was described by the amplitude-dependent variation of dynamic moduli ( $G'$ —elastic component and  $G''$ —viscous component) at constant frequency using the amplitude sweep. The structural characteristics of the samples within the linear viscoelastic (LVE) range were expressed by comparing the values of the  $G'$  and  $G''$  moduli. If  $G' > G''$ , the samples have gel-like behavior, and if  $G'' > G'$ , the samples have liquid-like behavior. The values of the dynamic moduli  $G'$  and  $G''$  allow to predict the properties of resistance to separation of paint components during long-term storage (Deka and Dey 2013; Eley 2005).

The analyzed paints have viscoelastic properties, which correspond to paste-like suspensions (figure S11, Supporting Information). The point of intersection between the  $G'$  elastic modulus and the  $G''$  loss modulus may be considered as a measure of the paint flow and dispersion capacity at small deformations. In the ECM and IAC samples (water-based products), the point of intersection occurs at low deformation values, which suggests a tendency to flow at low stresses, but  $G' > G''$  which have great importance for

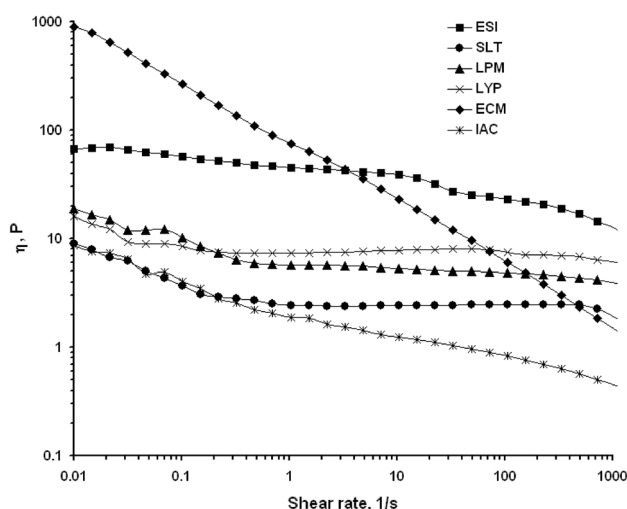


Fig. 7 Flow curves

flow resistance, explain the balance between paint coverage and runoff (Deka and Dey 2013).

The ECM paint sample shows  $G' > G''$  values and intersection point at higher deformation values compared to the IAC sample, thus highlighting its predominantly elastic behavior. The point of intersection at a higher deformation also indicates a higher value of the yield point. High values of yield point, which may be due to the presence of a large number of interactions (hydrogen bonds, etc.) between system components, indicate the ability of the paint to form a thicker film after application. In the IAC sample, with  $G' > G''$ , the intersection point occurs at a very low deformation value, which accounts for the lower stability to sedimentation compared to the ECM sample.

In the water-based paints (IAC, ECM), the viscoelastic solid behavior ( $G' > G''$ ) was observed, where as in the solvent-based paints (LPM, LYP, SLT, ESI) have the viscoelastic liquid behavior ( $G'' > G'$ ) (Table 1 —  $G'$  and  $G''$  values at 0.1% deformation). The values of the dynamic moduli recorded for the solvent-based samples suggest the existence of an instability of the composition over time (the

Table 1 Values of dynamic moduli at 0.1% deformation

Sample	$G'$ (Pa)	$G''$ (Pa)
IAC	2.367	0.881
ECM	181.038	83.705
LPM	2.546	5.507
LYP	2.813	6.486
SLT	2.265	2.579
ESI	7.060	29.391

Table 2 Pseudoplastic behavior determination using the Casson I model

Sample	Casson I model b
IAC	0.764
ECM	0.439
LPM	0.898
LYP	0.964
SLT	0.927
ESI	0.811

sedimentation phenomenon occurs); therefore, these paints should be very well stirred before application.

**Frequency sweep** The frequency sweep reveal the viscoelastic behavior of the analyzed samples (figure S12 Supporting Information). In the ECM sample, the high  $G'$  modulus values indicate the formation of a stable structure (gel-like behavior) due to enhanced bonds between the components of the system.

**Flow curves** Paints are subjected to different shear rates during manufacture, storage, dilution and application on surfaces. The flow curves represent the viscosity variation with shear rate and provide valuable information about the rheological behavior of the paints.

In the case of these paint samples, the flow curves obtained are specific to a pseudoplastic fluid with viscosity dependent on shear rate. The ECM sample has a more pseudoplastic behavior than other samples, which means the shear rate variation greatly influences viscosity values (Fig. 7) (Deka and Dey 2013). The Casson I model may be used to measure the pseudoplastic behavior of the samples (Table 2): Ostwald I model:  $y = a \cdot x^b$ ;  $x$ —input variable (shear rate);  $y$ —input variable (shear stress);  $a$ —factor;  $b$ —exponent.

According to Fig. 7, the viscosity of the ECM paint sample reaches a maximum value of 903 poise (P) when shear rate ranges between 0.01 and 0.1  $s^{-1}$ ; this range is specific to very low gravity force and vibrations. A high viscosity value within this shear rate range is specific to stable suspensions (the components do not separated over time) in storage conditions.

The viscosity values of the analyzed paints are low in the next measuring shear rate range (0.1–1  $s^{-1}$ ). This values indicate very good flow and uniform layer of the paint after it is applied on a surface. This low viscosity value is due to the decrease of the number of interactions between the system components.

**Time tests in oscillating and rotational mode** A slight instability over time was detected in the ECM paint when the rheological parameters of the sample ( $G'$  and  $G''$  dynamic moduli) were measured in oscillating mode (figure S13-a, Supporting Information). This drawback may be overcome by gently stirring the paint at certain time intervals, as evidenced by the rotational time test (Figure S13-b, Supporting Information), which clearly shows the structural stability of the analyzed paints at constant shear rate.

A rheometer can make shear rate measurements according to paint flow. The rate with which a paint is applied to a surface is of major importance in the formation of the paint film.

The rheological behavior of water-based paints must be very well controlled so that paints with the best possible rheological characteristics may be obtained. As shown in Table 3, the best paint films are achieved only when paint viscosity is controlled at each stage of the process (the ECM and ESI samples have a good stability over time and, after they have dried, an uniform film of paint and minimum run-off are achieved). Therefore, a good understanding and effective control of paint rheology are essential for high quality surface coating.

**Table 3** Important rheological parameters (Hester and Squire 1997) for achieving a thin and even paint film

	Shear rate ( $s^{-1}$ )	Reference viscosity range (poise)	Sample viscosity (Sample viscosity (poise))					
			IAC	ECM	LPM	LYP	SLT	ESI
Storage	0.1	> 100	4.06	265.7	10.15	8.45	3.67	57.36
Drying with good coverage and minimum deposits	1	50 ÷ 100	1.88	74.86	5.72	7.34	2.45	45.1
Transfer on the brush and no dripping	20	> 25	1.10	14.89	5.14	7.94	2.44	31.92

**Table 4** Parameters calculated based on the MCC tests

Sample	Mass (mg)	Residue (mg)	Char yield (wt%)	Decomposition rate (%)	THR (kJ/g)	HRC (J/(g.k))
ESI	3.92	0.63	16.07	83.93	17.36	113.44
LPM	2.56	0.40	15.63	84.37	16.75	143.09
SLT	4.59	0.21	4.58	95.42	19.48	154.73
LYP	4.70	0.52	11.06	88.94	22.20	236.66
ECM	3.88	0.34	8.76	91.24	15.63	236.73
IAC	3.24	0.66	20.37	79.63	5.86	84.60

The rapid restoration of the structure after application helps to avoid the runoff phenomenon, but affects the degree of coverage of these paints. This drawback may be overcome by adjusting the viscosity by optimizing the amount of rheological additives included in the paint (Eley 2005). Due to the use of water as a solvent, viscosity will be very low if no thickeners are used. Any water-based coating product must have a pseudoplastic behavior. This behavior accounts for the better performance of water-based paints compared to solvent-based paints (Xu 2005).

In conclusion, the market success of product depends on its formulation, and its rheological behavior may underline its suitability for a particular purpose. The correct formulation and choice of components allow the product to flow easily (yield point,  $\tau_0$ ), can prevent sedimentation of solid particles during storage, can determine good stability (zero shear viscosity,  $\eta_0$ ) and good applicability on surfaces (pseudoplastic behavior). Moreover, certain properties of the paint film can be estimated, thus determining the occurrence of some uses of great interest for automotive industry but also for the constructions sector.

### Dry paints characterization

#### MCC studies

The study of the fire behavior of some dry varnishes and paints is extremely important, as it allows us to determine how they may be used indoors in order to have a minimal negative fire safety impact.

Research in the field deals with improving fire performance (reducing heat release, controlling flammability temperature, reducing the spread of flame) but also with identifying toxic gases released by their pyrolysis. Microscale combustion calorimetry (MCC) tests have been performed for a wide range of polymers (Lyon and Walters 2004). In our research, we used the microscale combustion

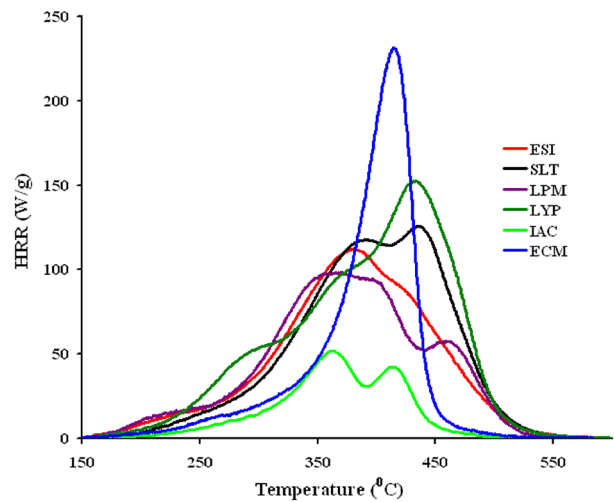


**Fig. 8** Temperature-dependent HRR curve representation for coating products

calorimetry (MCC) technique on dry paint films detached from wooden disks using a cutter, for the very first time. We analyzed samples with masses ranging from 2.5 to 4.7 mg. The tests allowed us to calculate a series of important parameters related to the fire behavior of the analyzed paints and varnishes. These parameters are: HRC—Heat release capacity; THR—Total heat released; char Yield—percentage of residual mass and decomposition rate—percentage of mass consumed during combustion. The results obtained are shown in Table 4.

Figure S14 of the Supporting Information shows HRC dependence on the amount of residue at the end of the test. The correlation was found to be very good, except for the SLT sample. A similar behavior was detected in THR dependence on the amount of residue. These findings confirm that the IAC sample has the best thermal stability during pyrolysis and the LYP sample has the poorest thermal stability. The LYP sample containing urea-alkyd resins has

**Table 5** Parameters extracted from the data provided by MCC

Sample	1			2			3		
	PHRR (W/g)	T <sub>PHRR</sub> (°C)	T <sub>imp</sub> (s)	PHRR (W/g)	T <sub>PHRR</sub> (°C)	T <sub>imp</sub> (s)	PHRR (W/g)	T <sub>PHRR</sub> (°C)	T <sub>imp</sub> (s)
ESI	112.05	385.28	237.50	–	–	–	–	–	–
LPM	98.55	370.13	228.00	57.70	459.88	318.50	–	–	–
SLT	117.69	387.45	227.50	125.61	431.13	271.50	–	–	–
LYP	57.41	323.67	175.00	106.84	398.60	250.50	152.55	439.05	291.50
ECM	231.23	411.32	271.50	–	–	–	–	–	–
IAC	51.92	363.20	219.50	42.50	413.99	270.50	–	–	–

1—the first peak heat release rate; 2—the second peak heat release; 3—the third peak heat release



a residue amount of 11.06%. It is one of the lowest values obtained for the samples that observe the linear dependence  $HRC=f(\text{Char yield})$  and one of the highest values for HRC, and also for THR. Linear dependencies between THR and char yield were obtained by Lin et al. (Lin et al. 2007) using MCC on a number of non-halogenated thermoplastic materials. They also found that, when halogens are present, THR is not influenced by the char yield variation. In our case, according to the manufacturers' statements, the SLT paint sample, which does not observe the linear dependence  $HRC=f(\text{Char yield})$ , contains halogens, i.e., Teflon (F).

The analysis of the results provided by MCC enabled us to calculate the parameters shown in Table 5, which also characterize the combustion process of the analyzed varnishes and paints: PHRR—Peak heat release rate;  $T_{\text{PHRR}}$ —Peak heat release rate temperature;  $T_{\text{imp}}$ —Peak heat release rate time. The first PHRR peak occurs after 175 s for the LYP sample, which confirms the lowest thermal stability during the pyrolysis process.

If one analyzes the graphical representations depending on temperature (Fig. 8) and on time (Figure S15 Supporting Information), one may note significant differences between the appearance of the curves and the number of peaks identified for the analyzed samples. The IAC and ECM samples are the extremes, as they have the lowest and highest HRC and PHRR, respectively.

Samples with one (ECM), two (LPM, SLT, and IAC) and three (LYP) peaks were found. The combustion virtually includes one, two or three stages, depending on the sample. This gradual degradation has also been found in other studies (Xu et al. 2016; Jin and Chung 2016). There are also notable differences as concerns the width of the curve; ECM and IAC, which are water-based coating products, have narrower curves (lower values for THR), while ESI, SLT, LPM and LYP, which are solvent-based varnishes and paints, have more extensive curves in both temperature and time range (higher THR). Thus, solvent-based varnishes and paints contribute more to the total amount of heat released during THR combustion (according to Table 4), thus supporting the spread of fire. There is also a similarity between the shape of the curve at the beginning of the combustion process and at its end between ECM and IAC (water-based coating products), and between ESI, SLT and LPM (solvent-based varnishes and paints). The LYP sample (urea-alkyd resin varnish), which is the only sample with 3 peaks, has the lowest peak heat release rate temperature ( $T_{\text{PHRR}}$ ), namely 323 °C, after the shortest time elapsed since the beginning of combustion (175 s) and releases the highest total amount of heat (THR). This sample may contribute the most to the development of a fire.

The ECM sample takes the longest, i.e., 271.5 s ( $T_{\text{imp}}$ ), to reach the highest temperature ( $T_{\text{PHRR}}=411.32$  °C of peak heat release rate (PHRR)=231.23 W/g, when the total heat

released (THR)=15.63 kJ/g is lower than in 4 other samples (LPM, ESI, SLT, LYP) and higher than in IAC.

As concerns the flammability of the substrate (wood) on which these varnishes and paints are applied, some researchers have shown that the ignition time is influenced by the amount of substance used, and by the number of coats (up to two coats of paint the ignition time increases by a factor of up to 2, and if the number of coats is increased by up to six the time decreases by a factor of up to 7) (Staggs et al. 2003). This means that no more than two coats of paint should be applied to increase the ignition time.

If we consider the TG/MS/FTIR results shown in the previous subchapter for all the types of varnishes and paints that we analyzed, carbon dioxide is the main combustion product at temperatures higher than 300 °C. Hydrocyanic acid was also released in the LYP sample.

According to the findings of our research, water-based paints should be preferred in small unventilated indoor locations, where there are users included in the risk categories (children, old individuals, bedridden individuals or individuals who cannot leave the premises by themselves). Solvent-based varnishes and paints contribute more to the total amount of heat released during THR combustion, thus supporting the spread of fire. The higher the amount of such coatings, the higher the risk of reaching dangerous concentrations of pyrolysis gases (Jodeh et al. 2020). Thus, when such varnishes and paints are used to achieve an aesthetic/architectural effect on wooden constructions, such as cabins, appropriate compensatory fire safety measures (fire prevention measures, high-performance pyrolysis gas detection systems, toxic gas exhaust systems, automatic extinguishing systems, etc.) should be taken when finishing protected wooden surfaces and inside the facilities where such substances are manufactured and stored.

## Conclusion

The TG/MS/FTIR technique used for analyzing the thermal behavior of certain commercial varnishes and paints has revealed that the degradation mechanism is complex and includes two to five decomposition stages depending on the composition. If we disregard the sample water or solvent evaporation stage, we find that the LYP sample containing urea-alkyd resins followed by the ECM and IAC samples, which also contain acrylic resins, have the lowest thermal stability. The best thermal stability was detected in the SLT sample-containing alkyd resins and Teflon. The MS and FTIR spectra obtained from the analysis of gas decomposition in air of water-based alkyd/acrylic resin (ECM) and water-based acrylic resin (IAC) paints indicate carbon dioxide as the major potentially harmful product. Benzene, xylene and carbon dioxide were the main potentially harmful



products in the solvent-containing coating products LYP, LPM, ESI, LPM, ESI and SLT. Hydrocyanic acid was also detected in the LYP sample containing urea-alkyd resins.

Rheological tests revealed a viscoelastic solid behavior in the water-based paints (IAC, ECM), and a viscoelastic liquid behavior in the solvent-based paints (LPM, LYP, SLT, ESI). The flow curves for all samples are specific of a pseudoplastic fluid with viscosity dependent on shear rate. The ECM sample has a more pseudoplastic behavior than the other samples, and the high  $G'$  modulus values indicate the formation of a stable structure (gel-like behavior) due to more bonds between the components of the system. The time tests in oscillating and rotational mode showed that the ECM and ESI samples enjoy good stability over time, and, after they have dried, an even coat and minimum runoff are achieved on the surface.

The MCC technique used on LYP sample revealed the lowest temperature of the first peak heat release rate ( $T_{PHRR}$ ), i.e., 323 °C, after the shortest time since the beginning of combustion (175 s) and releasing the highest total heat released (THR), which proves that this sample has the lowest thermal stability and may contribute the most to the development of a fire. MCC tests showed the best thermal stability during pyrolysis for the IAC sample, which also had the lowest HRC and THR values, and the highest amount of residue.

**Supplementary Information** The online version contains supplementary material available at <https://doi.org/10.1007/s13762-021-03579-6>.

**Acknowledgements** This work was supported by a grant of the Romanian Ministry of Research and Innovation, CCCDI—UEFISCDI, project number PN-III-P1-1.2-PCCDI-2017-0350 / 38PCCDI within PNCDI III. The authors Ion Anghel and Ioana-Emilia Șofran and are grateful for this financial support.

## References

- Crespi MS, Hikosaka MY, Amaral G, Ribeiro C (2007) Kinetic parameters obtained for thermal decomposition of acrylic resins present in commercial paint emulsions. *J Therm Anal Calorim* 88:669–672
- Deka A, Dey N (2013) Rheological studies of two component high build epoxy and polyurethane based high performance coatings. *J Coat Technol Res* 10:305–315
- Duce C, Bernazzani L, Bramanti E, Spepi A, Colombini MP, M.R. (2014) Tiné Alkyd artists' paints: Do pigments affect the stability of the resin? A TG and DSC study on fast-drying oil colours. *Polym Degrad Stabil* 105:48–58
- Eley RR (2005), Applied rheology in the protective and decorative coatings industry, *Rheology Reviews* 172–240.
- Gawdzik B, Rogulska M, Grochowicz M, Osypiuk-Tomasik J (2019) Studies of thermal properties of di(methacryloyloxymethyl) naphthalene–divinylbenzene (DMN–DVB) copolymer and its alkyl-bonded derivatives. *J Therm Anal Calorim* 138:4385–4393. <https://doi.org/10.1007/s10973-019-08150-7>
- Germinario G, van der Werf ID, Sabbatini L (2016) Chemical characterization of spray paints by a multi-analytical (Py/GC–MS, FTIR,  $\mu$ -Raman) approach. *Microchem J* 124:929–939. <https://doi.org/10.1016/j.microc.2015.04.016>
- Guo X, Ge S, Wang J, Zhang X, Zhang T, Lin J, Zhao CX, Wang B, Zhu G, Guo Z (2018) Waterborne acrylic resin modified with glycidyl methacrylate (GMA): Formula optimization and property analysis. *Polymer* 143:155–163
- Hester RD, Squire DR (1997) Rheology of waterborne coatings. *J Coat Technol*. 69:109–114
- Hof F, Schäfer RA, Weiss C, Hauke F, Hirsch A (2014) Novel  $\lambda$ 3-Iodane based functionalization of synthetic carbon allotropes (SCAs) – common concepts and quantification of the degree of addition. *Chem Eur Journal* 20:16644–16651
- Jiao L, Xiao H, Wang Q, Sun J (2013) Thermal degradation characteristics of rigid polyurethane foam and the volatile products analysis with TG-FTIR-MS. *Polym Degrad Stabil* 98:2687–2696. <https://doi.org/10.1016/j.polymdegradstab.2013.09.032>
- Jin E, Chung Y-J (2016) Combustion characteristics of pinus rigida specimens treated with mixed phosphorus-nitrogen additives. *J Ind Eng Chem* 36:74–79
- Jodeh S, Chakir A, Massad Y, Roth E (2020) Assessment of PM2.5, TVOCs, comfort parameters, and volatile organic solvents of paint at carpenter workshop and exposure to residential houses in Deir Ballout in , Int. J. Environ. Sci. Technol. <https://doi.org/10.1007/s13762-020-02877-9>
- Lin TS, Cogen JM, Lyon RE (2007) Correlations between microscale combustion calorimetry and conventional flammability tests for flame retardant wire and cable compounds, International Wire & Cable Symposium, Proceedings of the 56th IWCS 176–185.
- Lisa G, Yoshitake Y, Michinobu T (2016) Thermal degradation of some ferrocene-containing poly(aryleneethynylene)s. *J Anal Appl Pyrol* 120:399–408. <https://doi.org/10.1016/j.jaap.2016.06.010>
- Lisa G, Hamciuc C, Hamciuc E, Tudorachi N (2019) Thermal degradation study of some poly(arylene ether nitrile)s by TG/MS/FTIR analysis. *Polym Test* 75:220–228. <https://doi.org/10.1016/j.polymertesting.2019.02.012>
- Liu X, Hao J, Gaan S (2016) Recent studies on the decomposition and strategies of smoke and toxicity suppression for polyurethane based materials. *RSC Adv* 6:74742–74756. <https://doi.org/10.1039/C6RA14345H>
- Lyon RE, Walters RN (2004) Pyrolysis combustion flow calorimetry. *J Anal Appl Pyrol* 71:27–46
- Ma Z, Wang J, Yang Y, Zhang Y, Zhao C, Yu Y, Wang S (2018) Comparison of the thermal degradation behaviors and kinetics of palm oil waste under nitrogen and air atmosphere in TGA-FTIR with a complementary use of model-free and model-fitting approaches. *J Anal Appl Pyrol* 134:12–24. <https://doi.org/10.1016/j.jaap.2018.04.002>
- Standard Test Method for Determining Flammability Characteristics of Plastics and Other Solid Materials Using Microscale Combustion Calorimetry, ASTM D 7309–07.
- Odochian L, Moldoveanu C, Maftai D (2014) TG–FTIR study on thermal degradation mechanism of PTFE under nitrogen atmosphere and in air. Influence of the grain size. *Thermochim Acta* 598:28–35
- Ploeger R, Scalalone D, Chiantore O (2008) The characterization of commercial artists' alkyd paints. *J Cult Herit* 9:412–419. <https://doi.org/10.1016/j.culher.2008.01.007>
- Ploeger R, Chiantore O, Scalalone D (2009) Thermal analytical study of the oxidative stability of artists' alkyd paints. *Polym Degrad Stab* 94:2036–2041. <https://doi.org/10.1016/j.polymdegradstab.2009.07.018>



- Ploeger R, Chiantore O (2013) Characterization and Stability Issues of Artists' Alkyd Paints. In *New Insights into the Cleaning of Paintings: Proceedings from the Cleaning 2010 International Conference*, Universidad Politecnica de Valencia and Museum Conservation Institute, edited by M. F.Mecklenburg, A. E. Charola, R. J. Koestler, Smithsonian Contributions to Museum Conservation. Washington, DC: Smithsonian Institution 89–95
- Scalarone D, Chiantore O (2008) Separation techniques for the analysis of artists' acrylic emulsion paints. *J Sep Sci* 27:263–274
- Spranceana A-C, Darie M, Ciaușu S, Tudorachi N, Lisa G (2017) Comparative analysis of thermal stability of building insulation materials. *Environ Eng Manag J* 16:2831–2842
- Staggs JEJ, Phylaktou HN, McCreddie RE (2003) The effect of paint on the ignition resistance of plywood and chipboard. *Fire Saf. Sci.* 7:617–628
- Thao L, Zhao G-B, Qian J, Y-k. Qin, (2010) TG–FTIR characterization of pyrolysis of waste mixtures of paint and tar slag. *J Hazard Mater* 175:754–761
- Tsuge S, Ohtani H, Watanabe C (2011) Pyrolysis-GC/MS data book of synthetic polymers pyrograms, thermograms and ms of pyrolyzates, Elsevier The Boulevard, Langford Lane, Kidlington, Oxford OX5 1GB, UK Radarweg 29, PO Box 211, 1000 AE Amsterdam, The Netherlands, 2011.
- Tudorachi N, Mustata F (2020) Curing and thermal degradation of diglycidyl ether of bisphenol A epoxy resin crosslinked with natural hydroxy acids as environmentally friendly hardeners. *Arab J Chem* 13:671–682. <https://doi.org/10.1016/j.arabjc.2017.07.008>
- Wilkie CA, Chigwada G, Gilman JW Sr, Lyon RE (2006) High-throughput techniques for the evaluation of fire retardancy. *J. Mater. Chem.* 16:2023–2030
- Worzakowska M (2017) TG/DSC/FTIR/QMS studies on the oxidative decomposition of terpene acrylate homopolymers. *J Therm Anal Calorim* 127:2025–2035
- Xu J (2005) Rheology of polymeric suspensions: Polymer nanocomposites and waterborne coatings - Dissertation, The Ohio State University, 2005.
- Xu Z, Yan L, Guo Z, Liu D (2016) Effect of Alkyd varnish on the thermal stability and static smoke properties of decorative wood. *Procedia Eng* 135:637–643. <https://doi.org/10.1016/j.proeng.2016.01.129>

